Biocybernetics and Biomedical Engineering
2011, Volume 31, Number 2, pp. 23–32

Development of a Drug Delivery System Using Microcapsules with Ultrasound

KOHJI MASUDA*

Tokyo University of Agriculture & Technology, Nakacho, Koganei, Tokyo, Japan

Micrometer-sized microcapsules collapse upon exposure to ultrasound. Use of this phenomenon for a drug delivery system (DDS), not only for local delivery of medication but also for gene therapy, should be possible. However, enhancing of efficiency of medication is limited because the capsules in suspension diffuse in the human body after injection, since the motion of the capsules in blood flow cannot be controlled. To control behavior of the microcapsules, an acoustic radiation force was introduced. We detected local changes in the microcapsule density by producing of acoustic radiation force in an artificial blood vessel. Furthermore, we theoretically estimated the conditions required for an active path selection of the capsules at a bifurcation point in the artificial blood vessel. We observed the difference in the capsule density at both in the bifurcation point and in alternative paths downstream of the bifurcation point for the different acoustic radiation forces. We also confirmed that the microcapsules are trapped against flow with the condition when the acoustic radiation force is more than the fluid resistance of the capsules. The possibility of controlling of the capsule flow towards a specific point in a blood vessel was demonstrated.

K e y w o r d s: microcapsule, acoustic radiation force, drug delivery, artificial blood vessel

1. Introduction

The phenomenon that microcapsules or microbubbles of micrometer size collapse upon exposure to ultrasound near their resonance frequency has been identified as a basis for a physical drug delivery system (DDS) [1–3]. To minimize side effects, medication should only affect the target area, not other parts of the human body. Although the majority of recent research on DDSs has been focused on gene transduction using gene vectors, this method takes time and its development is costly. While the lifetime of the microbubbles is several minutes, the microcapsules, which

* Correspondence to: Kohji Masuda, Tokyo University of Agriculture & Technology, 2-24 Nakacho, Koganei, Tokyo, 184-8588 Japan, e-mail: masuda_k@cc.tuat.ac.jp
Received 26 January 2011; accepted 02 March 2011

can contain a specific drug inside a shell, are suitable for use with various types of medication. Furthermore, microcapsules are easily detected [4] and actuated [5, 6] by ultrasound. The distribution of capsules inside the body is easy to determine by echogram (B-mode image) because the brightness of echogram varies depending on the capsule density. We have developed software to detect local changes in the capsule density using the variation in brightness of an echogram [7]. Figure 1 shows a microscope image of F-04E microcapsules (Matsumoto Oil), which we used in this work.

However, because of the diffusion of capsules after injection, it is difficult to enhance the efficiency of medication. If behavior of the capsules could be controlled, the amount of medication required would be minimized. Microbubbles aggregate in water owing to Bjerknes forces, [5, 8, 9] which are produced by an ultrasound pressure gradient and oscillation of the diameter of the microbubbles. Since the oscillation of microcapsules is smaller than that of microbubbles, because of microcapsule shell, a microcapsule is thought to receive an acoustic radiation force [10–12] and be propelled by the acoustic propagation. In this paper, we describe our attempt for active path selection of the microcapsules in an artificial blood vessel by the acoustic radiation force.

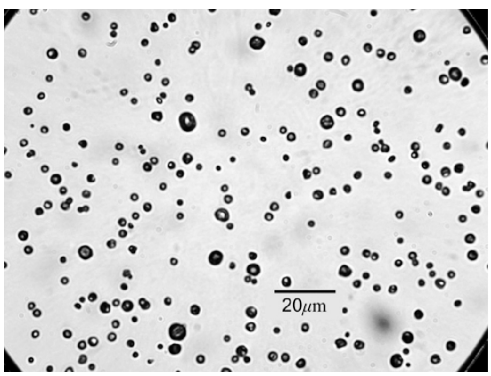

Fig. 1. Microscope image of F-04E microcapsules

2. Theory

Assuming spherical shape of the microcapsules, an acoustic radiation force F_{ac} [N] [13] acts to propel the capsules in the direction of acoustic propagation as per the following equation:

$$F_{ac} = \pi r^2 Y_p P \tag{1}$$

where P [W s/m^3] is the mean energy density of the incident wave, Y_p is a dimensionless factor called the radiation force function that depends on the scattering and

absorption properties of the capsule, and r [m] is the radius of the capsule. Here, the effect of ultrasound frequency in F_{ac} is not clear because Y_p does not include an item of frequency. When the microcapsules are placed in a flow, a capsule should receive a flow resistance F_d [N] as according to the following equation:

$$F_d = 6\pi r \mu u_r \tag{2}$$

where u_r [m/s] is velocity caused by the acoustic radiation force and μ [Pa s] is viscosity coefficient of the medium. Thus, if ultrasound is directed at a microcapsule in flow, and the acoustic radiation force is greater than the flow resistance, the trajectory of the capsule is curved, as shown in Fig. 2.

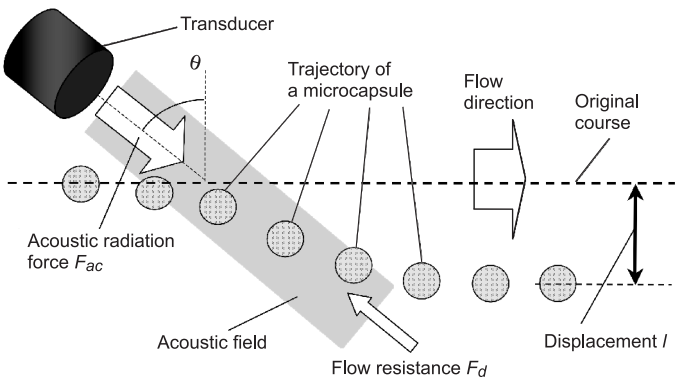

Fig. 2. Trajectory of the microcapsule in flow under ultrasound emission

When the microcapsules pass through an acoustic field where the sound pressure is higher than that at other areas, the capsules are propelled away from their original course. At larger value of angle θ in Fig. 2, the capsule passes through the acoustic field for a longer period causing a larger displacement from the original course. In Fig. 2, although the shape of the acoustic field is expressed as a square, it is dependent upon the transducer and should be measured before the calculation of theoretical displacement.

3. Experiments

3.1. Evaluation of Active Path Selection of Microcapsules

We used the above-mentioned F-04E microcapsule, which has a shell made of polyvinyl chloride (PVC), a specific gravity of 0.0225, and an average diameter of 4.0 [μm]. It contains isobutene inside and is stable in room temperature. We selected only the microcapsules with a diameter less than 10 [μm]. We also have prepared an artificial

blood vessel made of polyethylene glycol (PEG), including a Y-form bifurcation as shown in the schematic view of Fig. 3. The external size was 50 × 80 × 10 [mm^3] and the inner diameter of the paths was 2 [mm]. The blood vessel was placed in the bottom of a water tank, which was filled with water. Because the acoustic impedance of PEG is similar to that of water, the energy of ultrasound in water reaches the path with high efficiency. Using an inverted microscope (Leica, DMRIB), optical images of the observed areas 1 and 2 indicated in Fig. 3 were recorded independently.

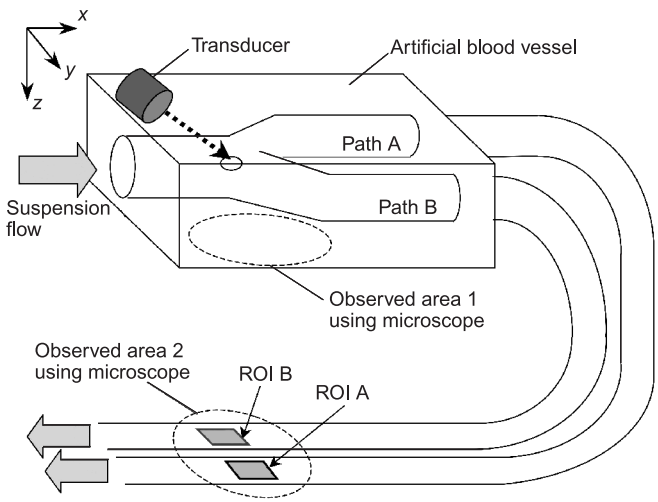

Fig. 3. Configuration of the artificial blood vessel, transducer, and two observed areas using microscope to evaluate active path selection of the microcapsules

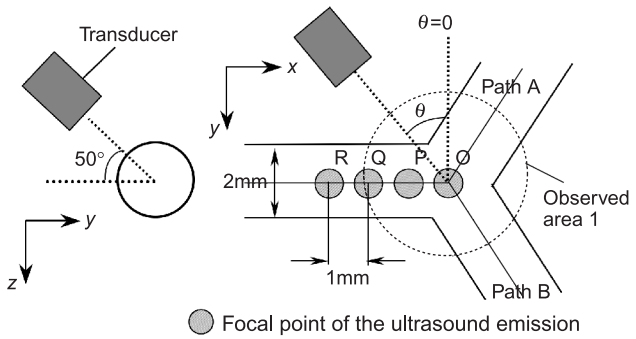

Fig. 4. Relationship between focal points of ultrasound and the bifurcation in the observed area 1

Figure 4 shows the relationship between focal areas of ultrasound and the bifurcation in the observed area 1. The axis of the transducer was set at 50 degrees counterclockwise to the x-axis and θ deg clockwise to the z-axis to prevent physical

interference between the transducer and the edge of the water tank. The transducer included a concave ceramic disc of diameter of 25 [mm]. Ultrasound was emitted by amplifying a sinusoidal signal from 0.5 to 2 [MHz] where the focal area of ultrasound is created in 60 [mm] from the surface of the transducer with a half width of sound pressure of 8 [mm].

Defining point O as the intersection of the three paths in Fig.4, the points P, Q, and R indicate points 1, 2, and 3 [mm] upstream from O, respectively. We observed behavior of the capsules in the observed area 1 upon injection of the capsule suspension at flow velocity of 200 [mm/s]. When ultrasound was emitted, more capsules entered path B than path A, whereas no significant difference was observed without ultrasound emission. Figure 5 shows the microscope images of the observed area 1 when the capsule suspension was injected and ultrasound of central frequency 2 [MHz] was focused at point Q with maximum sound pressure 400 [kPa]. Since stream of capsules were observed as a shadow, the possibility of active path selection of the capsules was clearly indicated. Here we confirmed that the capsules were not destroyed by the ultrasound since the frequency used was far from the resonance frequency of the capsules.

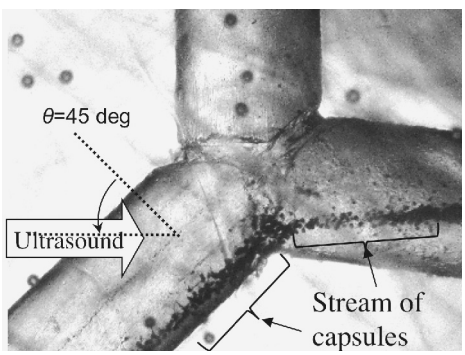

Fig. 5. Microscope image of the observed area 1 when injection of the capsule suspension during ultrasound emission

To evaluate a number of capsules that passed through each path, we extended two paths using semitransparent tubes and established an observed area 2, where both paths were observable in a single view, as shown in Fig. 3. Figure 6 shows microscope images of the observed area 2, which were captured using a high-speed camera (Casio, EX-F1) attached to the microscope with an interval time of 3.3 [ms] (300 [fps]), when the capsule suspension was injected with flow velocity of 5 [mm/s] with ultrasound emission of 2 [MHz] and maximum sound pressure of 500 [kPa]. Because of the limitation of optical magnification, though the individual microcapsules cannot be distinguished, thicker suspension in the path B is confirmed.

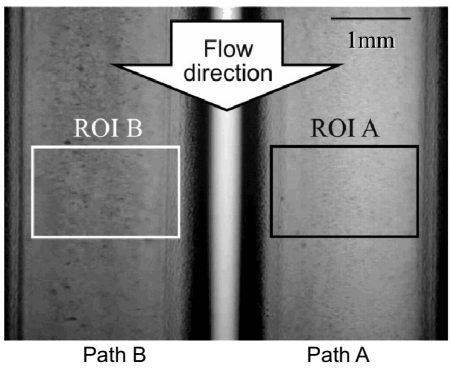

Fig. 6. Microscope images of the observed area 2 taken at 300 fps after injection of the capsule suspension with ultrasound emission

To measure the number of microcapsules, we established two square regions of interest in each path (ROIs A and B) and calculated the average brightness. The brightness (from 0 to 255) of a region decreases depending on the number of the capsules present. Thus, we defined the shadow index σ using the following equation to determine the number of the capsules in each ROI:

$$\sigma = \left(REF - \sum_{x} \sum_{y} f(x,y) \right) / REF \tag{3}$$

where f is the brightness of the ROI and REF is the summation of brightness in absence of the capsules in the ROI. Then, we confirmed the relation between the shadow index and the capsule density. The capsule suspension was passed through the ROI without ultrasound and the average of the shadow index for 15 frames (duration 30 [ms]) was calculated for various flow velocities. When the capsule density was 0.15–0.25 [g/L], significant changes in the density were detected [14].

3.2. Trapping Microcapsules Against Flow

To observe the behavior of the microcapsules if the acoustic radiation force propels the microcapsules against the flow, we have prepared an artificial blood vessel including a straight path as in the schematic view shown in Fig. 7. The external size is $55 \times 80 \times 10$ [mm^3] and the inner diameter of the path is 2 mm. It is placed in the bottom of a water tank, which is filled with water. By using an optical microscope (KH-7700, Omron, Japan), behavior of the microcapsules is observed and recorded.

We introduced two transducers, which were the same as used for active path selection, focused at the same point with their plane of incidence angle 2θ as shown in Fig. 7. The plane which includes axes of the transducers was set $\varphi = 50$ deg to prevent physical interference between the transducer and the edge of the water

tank. We produced several kinds of ultrasound waveform by varying of PRF (pulse repetition frequency) and duty ratio, which ranged 10, 20 and 50 [kHz], and 40, 60, 80 and 100 [%], respectively. We adjusted the maximum sound pressure at the focal point to be 300 [kPa].

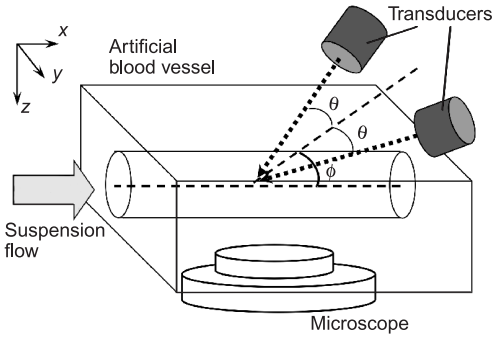

Fig. 7. Schematic view of the experiment to trap the capsules

Figure 8 shows time series of the images of the observed area, when the suspension was injected at 20 [mm/s]. Injection was finished within 10 [s]. In 20 [s] after injection aggregations of 100 [μm] were confirmed through the thick suspension. In 80–90 [s] the size of the aggregation saturated. As long as behaviors of the microcapsules were observed through the experiments, the reproducibility in shape, number and motion of the aggregations was poor. However, total occupied area of the microcapsules was seemed to increase with the duty ratio, which indicates that amount of the microcapsules increases in proportion to the duration of ultrasound emission.

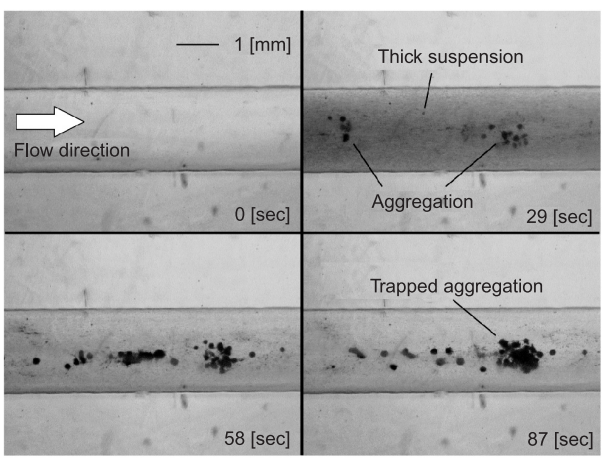

Fig. 8. Time series of the images of the observed area after injection of the suspension with ultrasound emission

4. Results

4.1. Evaluation of Active Path Selection of Microcapsules

We measured the shadow indices in two ROIs upon emission of sinusoidal ultrasound of frequency of 0.5 and 2 [MHz], and flow velocity of 5, 10 and 20 [mm/s]. Through the results obtained when ultrasound was focused at point Q shown in Fig. 4, the most significant path selection was indicated. Figure 9 shows ratio of the shadow index of ROI B to the summation versus the sound pressure at the bifurcation, where θ was fixed as 45 degree with the focused point Q. In Fig.9, the ratio more than 50% indicates that more capsules passed through path B than path A. When the frequency is 2 [MHz], the clear capsule selection to path B was confirmed. When the focal point was set at O, no significant difference was observed.

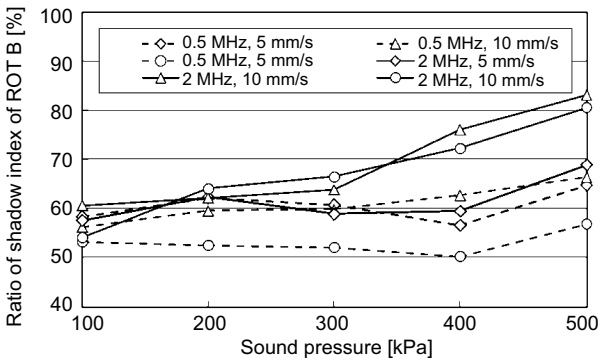

Fig. 9. Ratio in shadow index of ROI B to the summation (ROI A and B) with $\theta = 45$ degree

With sound pressure higher than 400 [kPa], 80% of capsules were introduced to a desired path, which result showed higher ability of path selection than our previous attempt [15] using a focused ultrasound. For active path selection of the capsules, higher pressure, higher frequency and plane ultrasound should be required.

4.2. Trapping of Microcapsules Against Flow

By referring the above condition, we recorded the microscope image when the size of the capsules is saturated under ultrasound emission. To evaluate amount of the trapped microcapsules quantitatively, we measured the occupied area of the microcapsules by a labeling method. Figure 10 shows the total occupied area of the trapped microcapsules from 0 to 87 [s] after ultrasound emission versus the duty ratio with PRF as a parameter. We confirmed that the area increases according to the duty ratio, where there was no significant difference in the PRF variation. Therefore duration of ultrasound emission is important to trap the microcapsules in the flow.

In many cases, aggregations of the microcapsules were seen upstream before they were trapped, which should be caused by Bjerknes forces [5, 8, 9] produced by an ultrasound pressure gradient and oscillation of the diameter of the microcapsules. We consider that an aggregation of the capsules makes equivalently a larger diameter capsule to receive more acoustic radiation force, which is proportional to the cube of the size of a microcapsule.

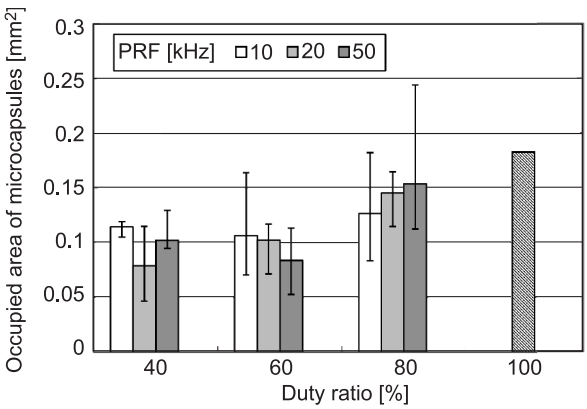

Fig. 10. Average of occupied area of trapped microcapsules versus duty ratio of ultrasound

5. Conclusions

In this study, we realized an active control of the microcapsules in an artificial blood vessel by acoustic radiation force. We confirmed that the capsules with a diameter less than 10 [μm] were directed into the desired path and were not destroyed by ultrasound of the applied sound pressures. Also we confirmed that the capsules were trapped against the flow when the flow velocity was less than that when the active path selection was observed. We are going to continue our research by varying other parameters of this experiment before commencing *in vivo* experiment. For further analysis, the precise conditions necessary to realize the active control of the capsules in a complicated shape of blood vessel should be elucidated.

References

1. Watanabe M., Chihara K., Shirae K., Ishihara K., Kitabatake A.: Pressure Measurement Using Ultrasonic Resonance of Microcapsules. Jpn. J. Appl. Phys.1991, 30, 1, 241–243.
2. Okada K., Kudo N., Niwa K., Yamamoto K.: A basic study on sonoporation with microbubbles exposed to pulsed ultrasound. J. Med. Ultrason. 2005, 32, 3–11.
3. Koyama D., Osaki A., Kiyan W., Watanabe Y.: Optical Observation of Microcapsule Destruction in an Acoustic Standing Wave. IEEE Trans. Ultrason. Ferroelect. Freq. Control 2006, 53, 1314–1321.

4. Ishihara K., Yoshii K., Chihara K., Masuda K., Shirae K., Furukawa T.: Path Lines in Blood Flow using High-speed Digital Subtraction Echography. Proc. IEEE Ultrasonic Symp. 1992, 1277–1280.
5. Yamakoshi Y., Koshiba M., Ozawa Y., Masuda N.: Trapping of Micrometer Size Bubbles by Ultrasonic Waves. Jpn. J. Appl. Phys. 2001, 40, 1526–1527.
6. Wei K., Skyba D.M., Firschke C., Jayaweera A.R., Lindner K.R., Kaul S.: Interactions between micro-bubbles and ultrasound: in viteo and in vivo observations. J. Am. Coll. Cardiol. 1997, 9, 1081–1088.
7. Yoshikawa H., Azuma T., Sasaki K., Kawabata K., Umemura S.: Dynamic and Precise Visualization of Contrast Agent in Blood Vessels with Motion Correction. Jpn. J. Appl. Phys. 2006, 45, 4754–4760.
8. Mitome H.: Micro Bubble and Sonoluminescence. Jpn. J. Appl. Phys. 2001, 40, 3484–3487.
9. Yamakoshi Y., Miwa T.: Microbubble Self-Trapping to Surface of Target. Jpn. J. Appl. Phys. 2008, 47, 4127–4131.
10. Kozuka T., Yasui K., Tuziuti T., Towata A., Iida Y.: Acoustic Standing-Wave Field for Manipulation in Air. Jpn. J. Appl. Phys. 2008,47, 4336–4338.
11. Lilliehorn T., Simu U., Nilsson M., Almqvist M., Stepinski T., Laurell T., Nilsson J., Johansson S.: Trapping of microparticles in the near field of an ultrasonic transducer. Ultrasonics 2005, 43, 293–303.
12. Zheng H., Dayton P.A., Caskey C., Zhao S., Qin S., Ferrara K.W.: Ultrasound-Driven Microbubble Oscillation and Translation Within Small Phantom Vessels. Ultrasound in Medicine and Biology, 2007, 33, 1978–1987.
13. Hasegawa T., Kido T., Min C.W., Iizuka T., Matsuoka C.: Frequency dependence of the acoustic radiation pressure on a solid sphere in water. Acoust. Sci. Technol. 2001, 22, 273-282.
14. Masuda K., Muramatsu Y., Nakamoto R., Ueda S., Nakayashiki Y., Ishihara K.: Active Path Selection of Fluid Microcapsules in Artificial Blood Vessel by Acoustic Radiation Force. Jpn. J. Appl. Phys. 2009, 48, 7, 07GK03.
15. Muramatsu Y., Ueda S., Nakamoto R., Nakayashiki Y., Masuda K., Ishihara K.: Active path selection of fluid microcapsules by acoustic radiation force in the artificial blood vessel, Proc. 4th European Medical & Biological Engineering Conference 2008, 1589–1593.